



Cite this: DOI: 10.1039/d1gc02490f

Si-Gly-CD-PdNPs as a hybrid heterogeneous catalyst for environmentally friendly continuous flow Sonogashira cross-coupling†

Francesco Ferlin,^{‡a} Daniele Sciosci,^{‡a} Federica Valentini,^a Janet Menzio,^b Giancarlo Cravotto,^{‡b} Katia Martina^{‡b} and Luigi Vaccaro^{‡*a}

We have reported a waste-minimized protocol for the Sonogashira cross-coupling exploiting the safe use of a CPME/water azeotropic mixture and the utilization of a heterogeneous hybrid palladium catalyst supported onto a silica/ β -cyclodextrin matrix in continuous flow. The use of the aq CPME azeotrope has proven to be crucial to enhance the catalyst performance including very low metal leaching. In addition, we have also completed the flow protocol by setting a downstream in-line liquid/liquid separation that allows the continuous recovery and reuse of the CPME fraction leading to consistent waste reduction. Finally, *E*-factor distribution and safety/hazard analysis have been performed highlighting the chemical and environmental efficiency of our protocol.

Received 13th July 2021,
Accepted 11th August 2021

DOI: 10.1039/d1gc02490f

rsc.li/greenchem

Introduction

Since its first appearance in the literature, the Sonogashira cross-coupling reaction¹ has been playing a pivotal role in organic synthesis. The formation of a new C–C bond between an acetylenic compound and an aromatic or aliphatic halide, in a fast and economical way, allows for the synthesis of several target compounds, *i.e.* active pharmaceutical ingredients as well as optoelectronic materials, with excellent yields.²

While the typical first discovered Sonogashira coupling is based on the use of a copper co-catalyst,^{1c} an effective, and nowadays interesting as more sustainable, copper-free approach was immediately disclosed by Cassar and Heck.^{1a,b} Currently, still considering sustainability issues, copper-free Sonogashira coupling (or the Cassar/Heck reaction) is desirably performed using recoverable catalytic palladium systems. Accordingly, the demand for newly developed heterogeneous catalysts for cross-coupling³ and in general for metal catalysed C–C bond formation processes⁴ is in continuous growth.³ Indeed, a more sustainable approach to prepare the desired

compounds with the possibility of easily removal and reuse of the metal-based catalytic systems is highly desirable.

Since the 90s, hybrid catalytic systems, that consist of both inorganic and organic components, have been employed in a wide range of reactions.⁵ Hybrid catalysts combine heterogeneous and homogeneous advantages with the key possibility to tune the hybrid materials making them suitable for different catalytic pathways and conditions.⁶

The preparation of organic–inorganic hybrid systems can be approached in two ways. The first, and most used, consists of a grafting procedure which is accomplished by physical adsorption. However, in this case, a non-homogeneous dispersion of the organic layer can be observed.⁷ The second approach is based on the selective covalent grafting between the organic and the inorganic components and it represents a valid alternative to preserve the structure, morphology and porosity of the support material.⁸

The most explored supports are mesoporous materials,⁹ polymers,¹⁰ nanostructures¹¹ and metal organic frameworks (MOFs),¹² while, the organic moiety can be a small molecule, or an oligomer and represent the anchored ligand. β -Cyclodextrins (β -CDs) can be efficiently used as ligand/stabilizers for metal nanoparticles.¹³ Due to their ability to host and stabilize metal ions and salts, CDs have been widely exploited for the preparation of hybrid organic–inorganic heterogeneous catalytic systems.¹⁴

Although, different heterogeneous catalysts and technologies have been developed to increase the efficiency of the Sonogashira reaction,¹⁵ the use of continuous flow methodologies is relatively less explored.¹⁶ When using a hybrid cata-

^aLaboratory of Green S.O.C. – Dipartimento di Chimica, biologia e Biotecnologie, Università degli Studi di Perugia, Via Elce di Sotto 8, 06123 – Perugia, Italy.

E-mail: luigi.vaccaro@unipg.it; <http://greensoc.chm.unipg.it/>

^bDipartimento di Scienza e Tecnologia del Farmaco, University of Turin, Via P. Giuria 9, 10125 Turin, Italy

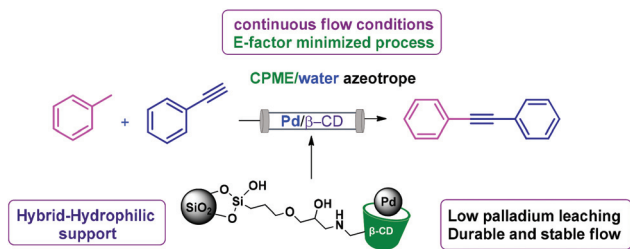
†Electronic supplementary information (ESI) available. See DOI: 10.1039/d1gc02490f

‡These authors contributed equally.

lytic system the use of flow conditions becomes of crucial utility where improved stability and recoverability of the solid catalyst can be achieved.^{17,18} In this regard, also the solvent selection plays a pivotal role in the efficiency of the whole strategy. Indeed, as demonstrated, it is possible to minimize metal leaching from a heterogeneous catalyst and expand its stability and use by a careful choice of the most appropriate solvent or solvent mixture.¹⁹

In this context, low-coordinating reaction media or azeotropic mixtures can be the preferred choice. Moreover, the latter can also be in certain cases recyclable leading to a dramatic minimization of waste.²⁰

In this contribution, after comparing a large number of potentially green and efficient reaction media, we focused our attention on the aqueous cyclopentyl methyl ether (CPME) azeotrope. This medium proved to be crucial in influencing the catalytic performance of the hybrid Si-Gly-CD-PdNPs- β -CD heterogeneous catalyst. Indeed, taking advantage of the hydrophilic nature of β -CD ligands, an easier access to the active catalytic sites occurs. Moreover, the presence of CPME and water allowed to solubilize both the reagents and the halide salts stoichiometrically produced during the process and leading to a homogeneous reaction mixture that can be processed in flow. Finally, we have also completed the protocol by combining a downstream in-line liquid/liquid continuous separation that allowed to efficiently recover and reuse the CPME fraction facilitating the work-up and minimizing waste-generation (Scheme 1).



Scheme 1 Features of Si-Gly-CD-PdNPs and β CD catalysed Sonogashira reaction in continuous flow.

Results and discussion

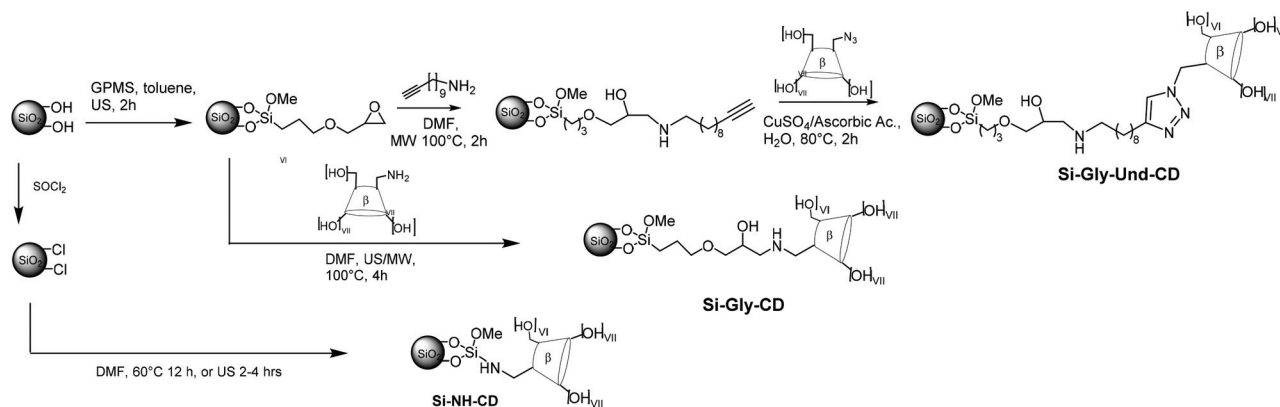
Our investigation began with the design and the preparation of a hybrid organic–inorganic support for supporting palladium nanoparticles (Pd NPs). Silica SIPERNAT 320 (Evonik) was employed as an inorganic support, having moderate adsorption capacity and a BET specific surface area (SSA) of $164 \text{ m}^2 \text{ g}^{-1}$.

Former studies showed that the Si-Gly-Und-CD support proved efficient and homogeneous impregnation of small Pd NPs exhibiting excellent activity.^{14g} It was demonstrated that an amino alcoholic spacer and the β -CD derivative effectively immobilize and stabilize Pd NPs thanks to the chelating and inclusive properties making both groups elemental for Pd anchoring. Its preparation started with derivatizing silica with 3-glycidoxypropyltrimethoxysilane (GPMS), which was then reacted with 10-undecynyl-1-amine (Und) to obtain an alkyl hydroxyl amino spacer prior to anchoring β -CD through a Cu-catalyzed azide–alkyne cycloaddition with 6¹-monoazido-6¹-deoxy- β -CD (Scheme 2).²¹

Aiming at simplifying the already established system (Si-Gly-Und-CD) in terms of synthetic steps, two different hybrid supports were also designed: a Si-Gly derivative was grafted with 6¹-amino-6¹-deoxy- β -CD which opened the epoxide ring reducing the length of the hydroxyl amino spacer (Si-Gly-CD); afterwards a third support was achieved consisting of β -CD directly bound to silica previously converted to silica chloride using thionyl chloride, followed by nucleophilic substitution with 6¹-amino-6¹-deoxy- β -CD (Si-NH-CD) (Scheme 2).

As reported in previous studies,^{14e} the beneficial effect of ultrasound (US) irradiation was exploited to maximize the grafting of GPMS and the synergic effect of combined MW and US irradiation was used when the Si-Gly derivative was reacted with 6¹-amino-6¹-deoxy- β -CD²¹ achieving an efficient grafting of β -CD in 4 h at 100°C . The reaction in the absence of enabling technologies required 16 h to reach the same results.

The synthesized silica derivatives were characterized by infrared spectroscopy (IR) and the grafting efficacy was measured from the percentage weight loss by thermogravimetric analysis (TGA) performed in the selected tempera-



Scheme 2 Synthetic routes to solid supported CDs Si-Gly-Und-CD; Si-Gly; Si-NH-CD.

ture range from 150 °C to 800 °C to negate the influence of solvents in the yield measure.

Different batches of directly grafted Si-NH-CD were prepared and despite the fact that the Si-Cl intermediate was always titrated before the reaction with β -CD we observed a limit in reproducibility. TGA analysis showed a constant decomposition of the sample, therefore we could not evidence any degradation step. Differently, as showed in Fig. 1, the first derivative peak temperature of Si-Gly-Und-CD was detected at 309 °C while the second was at 549 °C and a comparable trend was evidenced for Si-Gly-CD that starts the first thermal degradation at 319 °C while a second was detected at 489 °C. The results collected from different preparations of Si-Gly-Und-CD and Si-Gly-CD demonstrated a good reproducibility of grafting efficiency. As described in Table 1 the efficiency of grafting was measured on the basis of weight loss by TGA by comparison of different synthetic steps. The amount of loaded β -CD measured was from 57 to 130 $\mu\text{mol g}^{-1}$ in the three derivatives.

The quantification of grafted β -CD with unchanged inclusive properties was evaluated by loss of UV absorbance at 553 nm of phenolphthalein (Php) when included in the β -CD cavity after the treatment of a Php water solution with a weighed amount of β -CD-silica.^{14f} The high specificity of this titration highlights only the CDs available for the formation of the complex and we could observe differences when a spacer is used to maintain the inclusive capacity of cyclodextrin, therefore Si-Gly-Und-CD showed from the titration with PhP a comparable loading with respect to the TGA.

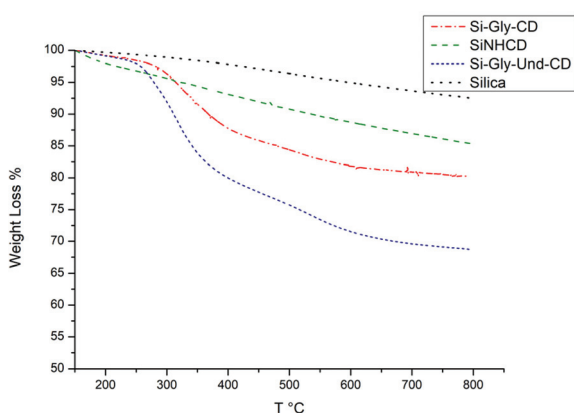


Fig. 1 TGA profiles of silica and organic-inorganic silica derivatives (a) Silica, (b) Si-NH-CD, (c) Si-Gly-CD, (d) Si-Gly-Und-CD.

Table 1 Loading quantification of grafted silica derivatives

Support	Loading % w/w	Loading $\mu\text{mol g}^{-1}$
Si-Gly	6.373 ^a	275 ^a
Si-Gly-CD	6.39 ^b -1.94 ^c	57 ^b -17 ^c
Si-Gly-Und-CD	17.2 ^b -9.3 ^c	130 ^b -83 ^c
Si-NH-CD	6.9 ^b -0.75 ^c	70 ^b -7 ^c

^a Gly amount measured by TGA. ^b β -CD grafting measured by TGA. ^c β -CD grafting measured by PhP titration.

The infrared spectrum of hybrid Si- β CD supports (see ESI†) shows the fingerprint modes of CD between 1500 and 1250 cm^{-1} (δCH and δOH bending modes). The intense CH/CH_2 stretching modes ($\nu\text{CH}/\text{CH}_2$) at 2928 and 2856 cm^{-1} prove the presence of an alkyl chain in Si-Gly-CD and in Si-Gly-Und-CD. The broad absorption between 3000 and 3750 cm^{-1} is related to $-\text{OH}$ groups from the CD rings and Si-OH groups from the silica surface (see ESI†). The νNH band at 1660 cm^{-1} can be seen and the IR spectrum of Si-Gly-Und-CD showed also a band at 1630 with a shoulder that corresponds to the triazolyl group ring vibrations.

PdNPs were immobilized on the supports by reduction of the $\text{Pd}(\text{OAc})_2$ precursor in ethanol with heating at reflux.

From the inductively coupled plasma (ICP) analyses carried out on the catalysts, palladium loading data were obtained (Table 2). The results showed that all the Si-CD supports load Pd NPs efficiently.

All three catalysts were preliminary tested in a C-C Heck coupling reaction to evaluate if comparable catalytic activities could be observed. As previously optimized, styrene may efficiently react with iodo-benzene in the presence of 0.5 mol% Pd NPs supported on Si-Gly-Und-CD at 120 °C in MW for 1 h.^{14g} The reaction gave successfully >99% on conversion with both Si-Gly-Und and Si-Gly-CD supported Pd nanocatalysts. 82% conversion was observed with Si-NH-CD (see ESI†). Although it enables comparable Pd adsorption this support showed limit in preparation reproducibility and lower synthetic activity therefore it was discarded. Since the **Si-Gly-CD-PdNPs** showed comparable reactivity, stability, and a reliable and simplified synthesis when compared to the Si-Gly-Und derivative, it was selected for tests carried out in this work. Surprisingly we observed that the inclusive capacity of CD does not affect the loading capacity of the Pd NPs and their catalytic activity.

TEM images of the catalysts Si-Gly-CD-PdNPs are shown in Fig. 2. The solid supported catalyst consists of uniform (mainly spheroidal) particles with a diameter range of 2–8 nm (Fig. 2, particle distribution). Surprisingly by comparison with the Si-Gly-Und-CD-PdNPs^{14g} already studied, we could observe that smaller Pd particles were present on Si-Gly-CD but with a comparable uniformity of distribution.

With the catalyst in hand, we started to test the catalytic performance in the model Sonogashira coupling between iodo-benzene **1a** and phenylacetylene **2a** in the presence of DABCO as a base. We screened environmentally friendly reaction media, different common petrol-based solvents, and their combination with water for the preliminary selection of the best reaction conditions (Table 3).

Table 2 PdNP loading (% w/w) from ICP analysis

Catalyst	Loading % w/w
Si-Gly-Und-CD-PdNPs	2
Si-Gly-CD-PdNPs	1.8
Si-CD-PdNPs	2.2

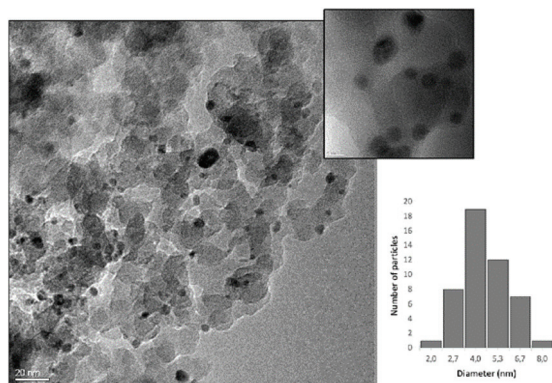
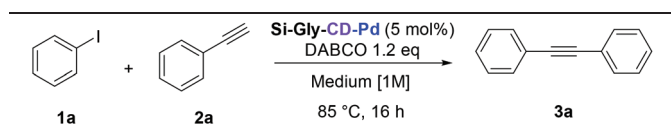


Fig. 2 TEM images of Si-Gly-CD Pd NPs. Pd particle size distribution is also reported.

Table 3 Screening of reaction media for Sonogashira cross-coupling of **1a**^a



Entry	Medium	C^b [%]
1	DMF	90
2	DMF/water (6 : 1)	92
3	DMF/water (2 : 1)	88
4	NMP	70
5	NMP/water (2 : 1)	73
6	CH ₃ CN	70
7	CH ₃ CN/water az.	85
8	Propylene carbonate	87
9	Ethylene carbonate	89
10	GVL	90
11	GVL/water (2 : 1)	92
12	2-Me-THF	87
13	CPME	85
14	CPME/water az.	97 (94) ^c
15	Water	74
16	Water + SDS	88

^a Reaction conditions: **1a** (1 mmol), **2a** (1.5 mmol), base (1.2 eq.), Si-Gly-CD-PdNPs (5 mol%), solvent (1 mL, 1 M), 85 °C, 16 h. ^b GLC conversion has been determined using samples of the pure compound as reference standards; the remaining materials are **1a** and **2a**. ^c Isolated yield is given in parenthesis.

The catalyst showed good performance in almost all the reaction media tested. The enhancement of the catalytic activity is interesting when a mixture of solvent/water was employed. This behaviour is attributable to the hybrid nature of our Si-Gly-CD-PdNP catalyst. Indeed, the presence of β -CDs makes the hybrid heterogeneous system water-friendly. It is worth noting that the benefits achieved from the presence of water are strictly related to its ratio with the organic solvent (see for example Table 3 entries 1–3).

Moreover, when the organic solvent and water form an azeotropic mixture, homogeneous or heterogeneous, the improvement in catalytic activity is remarkable. When pure

CH₃CN is used as a solvent 70% of product **3a** was obtained (Table 3, entry 6) while, in the CH₃CN/water azeotropic mixture the conversion increased up to 85% (Table 3, entry 7). The same increase was observed also for CPME (Table 3, entry 13) and CPME/water heterogeneous azeotropic mixtures (Table 3, entry 14) leading to 97% conversion of product **3a** with high isolated yield, further confirming the benefit related to the presence of water.

With the optimized reaction conditions, we proceeded to test the stability and durability of our catalyst in the selected reaction medium CPME/water azeotrope (Table 4).

As expected, the catalyst showed very promising results in terms of recyclability allowing to be reused for three representative consecutive runs without loss in catalytic efficiency, and up to five runs with negligible differences. Moreover, the catalyst was further stressed by performing recycling experiments at half conversion (Fig. 3) showing good durability.²²

With these promising results under batch conditions, we began to plan the assembly of our flow system. We packed the Si-Gly-CD-PdNP catalyst inside a stainless-steel reactor and we installed it into a thermostated box. The system has been designed by using two channels for the delivery of the reactant through the catalyst column (Fig. 4).

Table 4 Catalyst recycling and reuse under batch conditions^a



Run	C^b [%]	Leaching ^c (%)
1	97 (94)	0.94
2	97 (94)	0.86
3	97 (94)	0.86
4	95 (91)	0.84
5	88 (85)	0.82

^a Reaction conditions: **1a** (1 mmol), **2a** (1.5 mmol), DABCO (1.2 eq.), Si-Gly-CD-PdNPs (5 mol%), CPME/water az (1 mL, 1 M), 85 °C, 16 h.

^b GLC conversion has been determined using samples of the pure compound as reference standards; the remaining materials are **1a** and **2a**.

^c Determined with MP-AES, as percentage from the initial content of the fresh catalyst.

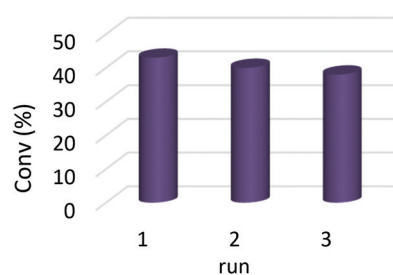


Fig. 3 Catalyst recycles at $t_{1/2}$ under batch conditions. Reaction conditions: **1a** (1 mmol), **2a** (1.5 mmol), catalyst (5 mol%), DABCO (1.2 eq.), solvent (1 mL, 1 M), 7 h.

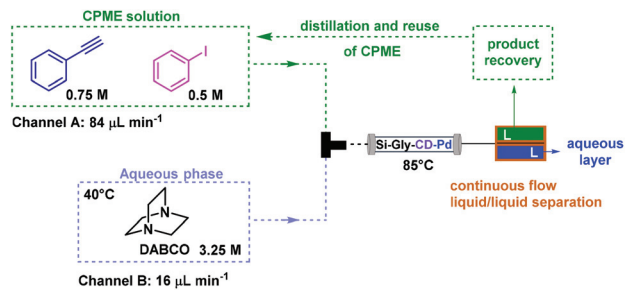


Fig. 4 Continuous flow system for the Sonogashira reaction.

The channel A was charged with a CPME solution of **1a** and **2a** (0.5 M and 0.75 M respectively) while channel B with a 3.25 M aqueous solution of DABCO and kept at 40 °C. The flow rates of the two channels have been regulated in order to have the exact azeotropic ratio of CPME/water inside the reactor (see the ESI† for further details).

Further optimizations of the other flow parameters were conducted to achieve a stable and durable conversion over the time (Table 5). When 100–250 BPRs were used, poor conversion was obtained associated with a low residence time (Table 5, entries 3 and 4), while, increasing the residence time to 35–50 minutes resulted in good to excellent conversions to product **3a** (Table 5, entries 5–7).

At the output of the reactor, a liquid/liquid membrane separator was installed for the separation of the reaction mixture in the two pure components. These features allow us to also optimize the work-up procedure. Indeed, by the evaporation and recovery of the CPME we were also able to reuse it continuously, while the aqueous DABCO-I solution represents the sole waste of the reaction.

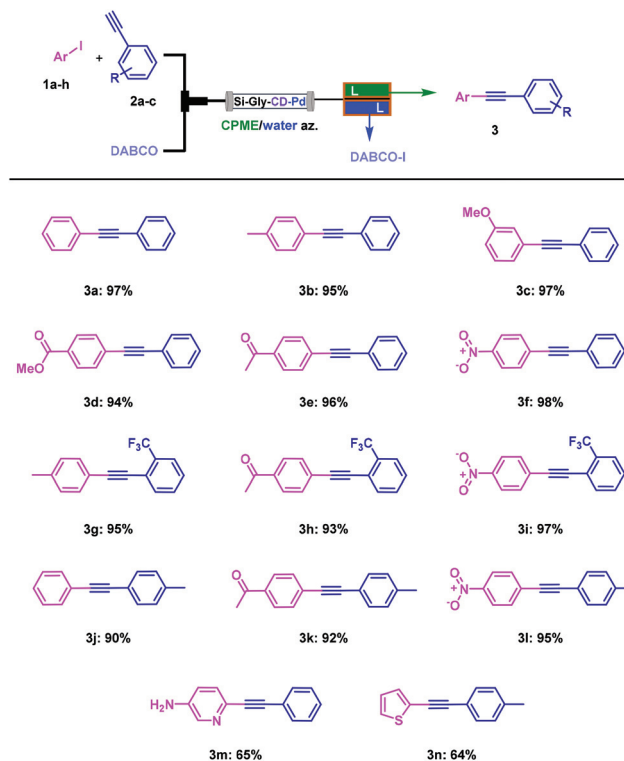
With the optimized continuous-flow set-up we started to explore the scope of the Sonogashira reaction achieving high yields for all the substrates screened (Scheme 3).

Both electron withdrawing and electron donating groups on the iodoarene are well tolerated as well as electron donating group in the acetylenic compound leading to excellent isolated

Table 5 Optimization of flow parameters

Entry	Channel A (mL min ⁻¹)	Channel B (mL min ⁻¹)	BPR (psi)	Residence time	C ^a [%]
1	0.840	0.160	500	10 min	9
2	0.420	0.080	500	20 min	48
3	0.420	0.080	250	7 min	3
4	0.420	0.080	100	5 min	3
5	0.168	0.032	500	35 min	60
6	0.084	0.016	500	50 min	99
7	0.084	0.016	250	40 min	93

^a GLC conversion has been determined using samples of the pure compound as reference standards; the remaining materials are **1a** and **2a**.



Scheme 3 Scope of Sonogashira in flow. Isolated yields are reported.

yields (90–98%). Moreover, our continuous flow set-up showed good performance also when iodo-heterocycles (**1g–h**) were coupled with phenylacetylene **2a** and deactivated alkyne **2c**.

By employing the designed flow set-up, we were able to efficiently convert 20 mmol of the differently substituted iodoarene, heterocycles and phenylacetylenes with only 0.06 mmol palladium (350 mg of Si-Gly-CD-PdNP catalyst) proving the catalyst stability and durability. Under these conditions, and after 10 h of continuous operation, the catalyst showed a TON value of 333 and a TOF of 33 h⁻¹.

In addition, the palladium leaching was continuously monitored during the flow operation (Fig. 5). The value recorded was extremely low in the first 5 h of flow procedure with an additional reduction over the next hours. TEM images of the used catalyst Si-Gly-used CD-PdNPs (see the ESI†) show that Pd NPs formed some nanoparticle agglomerates with a slightly increase in the particle size.

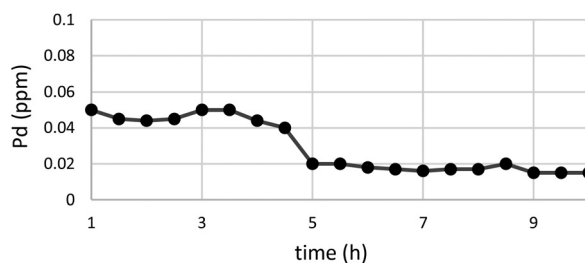


Fig. 5 Leaching of metal in solution.

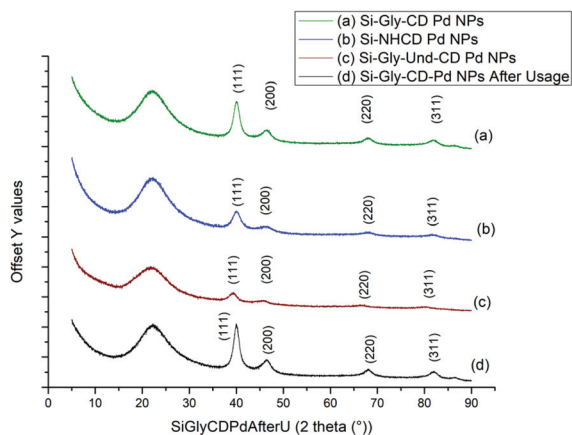


Fig. 6 XRD patterns measured on samples listed in Table 1: (a) Si-Gly-CD-PdNPs; (b) Si-CD-PdNPs; (c) Si-Gly-Und-CD-PdNPs and (d) Si-Gly-CD-PdNPs after usage.

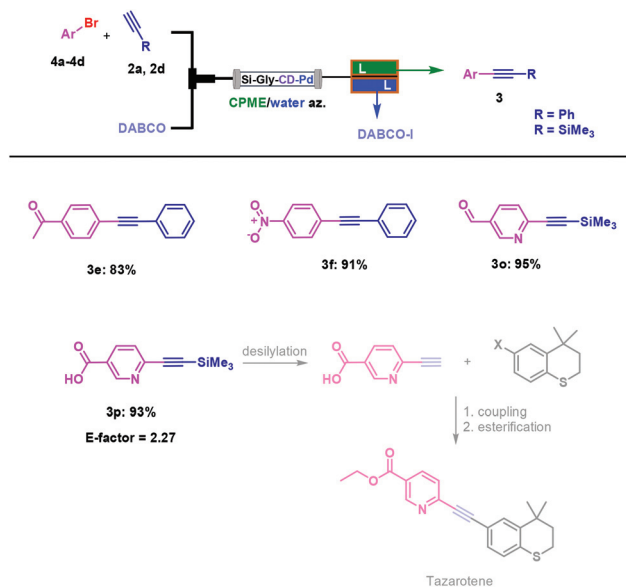
XRD patterns of the fresh catalysts (Fig. 6, pattern a, b and c) and of the catalyst used in the flow procedure (Fig. 6, pattern d) prove that Pd NPs exist on the Pd/Si-CD. As shown in Fig. 6, the typical diffused scattering of the amorphous SiO₂ support gave the strongest peak in the XRD pattern (21.868). The other peaks are indexed as the (111), (2 0 0), (2 2 0), and (3 1 1) planes of the Pd NPs (cubic phase, JCPDS 46-1043). With respect to standard references, a slight shift in the 2θ values was observed, for all peaks, and we can assume that a small increase in crystallite θ spacing happens as a consequence of the particle nano size.

In order to evaluate the efficiency of the catalyst utilized in the newly developed flow reactor, we have also tested more challenging aryl-bromides as substrates. Under identical conditions in flow aryl-bromide **4a** and **4b** gave high isolated yield of the corresponding coupling products. We therefore also finalized our study in the synthesis of API intermediates **3o** and **3p** obtained by coupling 6-Br-nicotinaldehyde **4c** and 6-Br-nicotinic acid **4d** with trimethylsilylacetylene **2d** (Scheme 4).

Compound **3p** is obtained with an *E*-factor of 2.27, and it is the key intermediate that by already reported procedures,²³ after desilylation and coupling with 6-halo-4,4-dimethylthiochromane allows to obtain the API tazarotene. Finally, in order to evaluate the sustainability improvement of our protocol, we focused our attention on a comprehensive and general assessment of the environmental features. Initially we calculated the mass-dependent metrics (*E*-factor) for the whole procedure and for other representative similar flow processes (Fig. 7). Due to the CPME recovery and reuse, the *E*-factor value associated with our flow set-up is extremely low (2.12).

Aiming at the identification of the major contributions to the very low *E*-factor values,²⁴ we observed that the mixture concentration and the auxiliary material strongly affected the waste production (see the ESI† for further details).

In addition, to gain more insight, we analysed different green metrics in terms of the vector magnitude ratio by adopting the radial polygon analysis (Fig. 8).²⁵



Scheme 4 Scope of Sonogashira in flow using aryl-bromide. Isolated yields are reported.

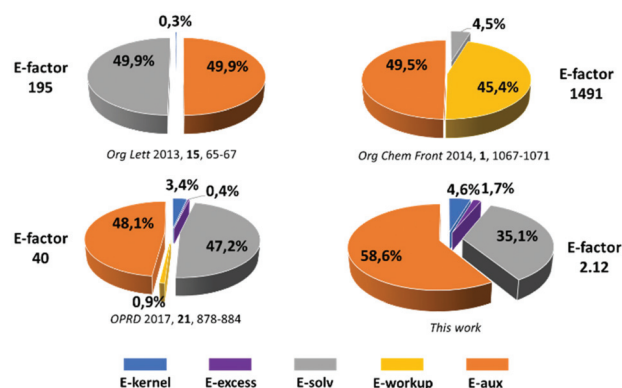


Fig. 7 *E*-Factor distribution analysis.

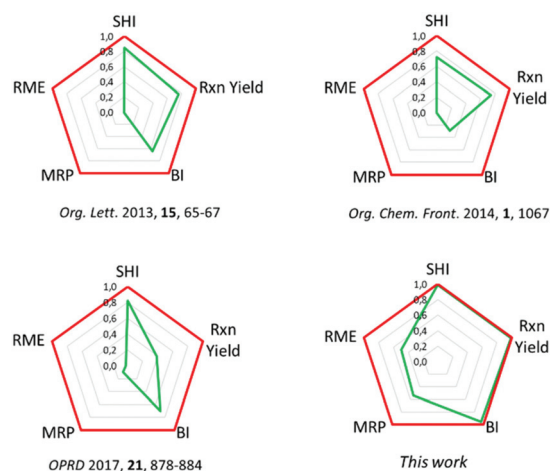


Fig. 8 Environmental and safety analyses based on radial polygons.

In these analyses we also have included the determination of the benign index (BI) and the safety hazard index (SHI) associated with the waste material.

This comparison highlights that the reuse of the solvent mainly influenced the environmental profile exploited by our flow assisted Sonogashira reaction. In addition, the BI and SHI highly benefit from the use of CPME as an environmentally friendly solvent and DABCO as the base, which has a higher flash point (62.2 °C) in comparison with triethylamine (−11 °C)^{16a} and diisopropylethylamine (9.5 °C),^{16d} and low vapour pressure (72 hPa at 23 °C).

Conclusions

In conclusion, here we reported a flow-assisted Sonogashira cross-coupling reaction catalysed by a Si-Gly-CD-PdNP hybrid catalyst. The catalytic efficiency was improved by exploiting the hydrophilicity of the β -CD ligand allowing the utilization of a CPME/water azeotropic mixture. The selected reaction medium and flow technology led to a dramatic minimization of metal leaching in solution, improving catalyst stability and durability.

Moreover, the synergy between the recovery of CPME and the packed-bed flow technology allows us to achieve great improvement in terms of waste reduction. The designed methodology allowed the continuous flow production of 20 mmol of differently substituted compounds with only 0.06 mmol palladium.

The environmental features were also evaluated based on the green-metrics and by considering the safety hazard and the benign index associated with the waste material.

Conflicts of interest

There are no conflicts to declare.

Acknowledgements

The Università degli Studi di Perugia and MIUR are acknowledged for financial support to the project AMIS, through the program “Dipartimenti di Eccellenza – 2018–2022”. The University of Turin is acknowledged for the financial support (ricerca locale 2020). We thank M. C. Valsania (Mayita) from the Microscopy Laboratory of the NIS Centre and Prof G. Berlier for their precious help.

Notes and references

- (a) H. A. Dieck and F. R. Heck, *J. Organomet. Chem.*, 1975, **93**, 259–263; (b) L. Cassar, *J. Organomet. Chem.*, 1975, **93**, 253–257; (c) K. Sonogashira, Y. Tohda and N. Hagihara, *Tetrahedron Lett.*, 1975, **50**, 4467–4470.
- (a) R. Chinchilla and C. Nájera, *Chem. Rev.*, 2014, **114**, 1783–1826; (b) R. Chinchilla and C. Nájera, *Chem. Soc. Rev.*, 2011, **40**, 5084–5121; (c) C. Torborg and M. Beller, *Adv. Synth. Catal.*, 2009, **351**, 3027–3043; (d) R. Chinchilla and C. Nájera, *Chem. Rev.*, 2007, **107**, 874–922.
- (a) I. Favier, D. Pla and M. Gomez, *Chem. Rev.*, 2020, **120**, 1146–1183; (b) A. Biffis, P. Centomo, A. Del Zotto and M. Zecca, *Chem. Rev.*, 2018, **118**, 2249–2295; (c) A. Molnar, *Chem. Rev.*, 2011, **111**, 2251–2320; (d) I. J. S. Fairlamb and N. W. J. Scott, *Pd Nanoparticles in C–H Activation and Cross-coupling Catalysis in Nanoparticles in Catalysis*, 2020, pp. 171–205.
- (a) A. Bavykina, N. Kolobov, I. S. Khan, J. A. Bau, A. Ramirez and J. Gascon, *Chem. Rev.*, 2020, **120**, 8468–8535; (b) D. Sciosci, F. Valentini, F. Ferlin, S. Chen, Y. Gu, O. Piermatti and L. Vaccaro, *Green Chem.*, 2020, **22**, 6560–6566; (c) S. Mujahed, F. Valentini, S. Cohen, L. Vaccaro and D. Gelman, *ChemSusChem*, 2019, **12**, 4693–4699; (d) F. Valentini, G. Brufani, L. Latterini and L. Vaccaro, *Metal Nanoparticles Catalyzed C–C Bond Formation via C–H Activation in Advanced Heterogeneous Catalysts Volume 1: Applications at the Nano-Scale*, 2020, pp. 513–543.
- (a) E. Heuson, R. Froidevaux, I. Itabaiana Jr., R. Wojcieszak, M. Capron and F. Dumeignil, *Green Chem.*, 2021, **23**, 1942–1954; (b) M. Kalaj, K. C. Bentz, S. Ayala Jr., J. M. Palomba, K. S. Barcus, Y. Katayama and S. M. Cohen, *Chem. Rev.*, 2020, **120**, 8267–8302; (c) M. Liras, M. Barawi and V. A. de la Pena O’Shea, *Chem. Soc. Rev.*, 2019, **48**, 5454–5487; (d) U. Diaz, D. Brunel and A. Corma, *Chem. Soc. Rev.*, 2013, **42**, 4083–4097.
- (a) E. D. Goodman, C. Zhou and M. Cargnello, *ACS Cent. Sci.*, 2020, **6**, 1916–1937; (b) Y. Wang, L. Chen, C.-C. Hou, Y.-S. Wei and Q. Xu, *Org. Biomol. Chem.*, 2020, **18**, 8508–8525; (c) Y. Ding, P. Zhang, H. Xiong, X. Sun, A. Klyushin, B. Zhang, Z. Liu, J. Zhang, H. Zhu, Z.-A. Qiao, S. Heumann and S. Dai, *Green Chem.*, 2020, **22**, 6025–6032; (d) R. Ye, J. Zhao, B. B. Wickemeyer, F. D. Toste and G. A. Somorjai, *Nat. Catal.*, 2018, **1**, 318–325.
- B. Lei, B. Li, H. Zhang, L. Zhang and W. Li, *J. Phys. Chem. C*, 2007, **111**, 11291–11301.
- M. Benzaqui, R. Semino, F. Carn, S. R. Tavares, N. Menguy, M. Giménez-Marqués, E. Bellido, P. Horcajada, T. Berthelot, A. I. Kuzminova, M. E. Dmitrenko, V. A. Penkova, D. Roizard, C. Serre, G. Maurin and N. Steunou, *ACS Sustainable Chem. Eng.*, 2019, **7**, 6629–6639.
- (a) N. Lashgari, A. Badiie and G. Mohammadi Ziarani, *Nanochem. Res.*, 2016, **1**, 127–141; (b) S. Singh, R. Kumar, H. D. Setiabudi, S. Nanda and D.-V. N. Vo, *Appl. Catal., A*, 2018, **559**, 57–74; (c) M. J. Ndolomingo and R. Meijboom, *Catal. Lett.*, 2019, **149**, 2807–2822; (d) D. Chen, P. Zhang, Q. Fang, S. Wan, H. Li, S. Yang, C. Huang and S. Dai, *Inorg. Chem. Front.*, 2018, **5**, 2018–2022.
- (a) A. Azeez, L. Polio, J. E. Hanson and S. M. Gorun, *ACS Appl. Polym. Mater.*, 2019, **1**, 1514–1523; (b) P. P. Fedorov, A. A. Luginina, S. V. Kuznetsov, V. V. Voronov, A. A. Lyapin,

- P. A. Ryabochkina, M. V. Chernov, M. N. Mayakova, D. V. Pominova, O. V. Uvarov, A. E. Baranchikov, V. K. Ivanov, A. A. Pynenkov and K. N. Nishchev, *J. Fluor. Chem.*, 2017, **202**, 9–18.
- 11 (a) N. Ahadi, M. A. Bodaghifard and A. Mobinikhaledi, *Appl. Organomet. Chem.*, 2019, **33**, e4738; (b) M. Fallahi, E. Ahmadi and Z. E. Mohamadnia, *Appl. Organomet. Chem.*, 2019, **33**, e4975.
- 12 (a) W. Li, Y. Zhang, Q. Li and G. Zhang, *Chem. Eng. Sci.*, 2015, **135**, 232–257; (b) P. T. Yin, S. Shah, M. Chhowalla and K.-B. Lee, *Chem. Rev.*, 2015, **115**, 2483–2531.
- 13 T. Skorjanc, F. Benyettou, J. C. Olsen and A. Trabolsi, *Chemistry*, 2017, **23**, 8333–8347.
- 14 (a) M. I. Velasco, C. R. Krapacher, R. H. de Rossi and L. I. Rossi, *Dalton Trans.*, 2016, **45**, 10696–10707; (b) G. Kurokawa, M. Sekii, T. Ishida and T. Nogami, *Supramol. Chem.*, 2004, **16**, 381–384; (c) L. I. Rossi, C. O. Kinen and R. H. de Rossi, *C. R. Chim.*, 2017, **20**, 1053–1061; (d) F. Calsolaro, K. Martina, E. Borfecchia, F. Chavez-Rivas, G. Cravotto and G. Berlier, *Catalyst*, 2020, **10**, 1118; (e) K. Martina, F. Calsolaro, A. Zuliani, G. Berlier, F. Chavez-Rivas, M. J. Moran, R. Luque and G. Cravotto, *Molecules*, 2019, **24**, 2490; (f) E. C. Gaudino, S. Tagliapietra, G. Palmisano, K. Martina, D. Carnaroglio and G. Cravotto, *ACS Sustainable Chem. Eng.*, 2017, **5**, 9233–9243; (g) K. Martina, F. Baricco, M. Caporaso, G. Berlier and G. Cravotto, *ChemCatChem*, 2015, **8**, 1176–1184; (h) K. Martina, F. Baricco, G. Berlier, M. Caporaso and G. Cravotto, *ACS Sustainable Chem. Eng.*, 2014, **2**, 2595–2603; (i) B.-H. Han and M. Antonietti, *J. Mater. Chem.*, 2003, **13**, 1793–1796; (j) S. Bahadorikhalili, L. Ma'mani, H. Mahdavi and A. Shafiee, *Microporous Mesoporous Mater.*, 2018, **262**, 207–216; (k) R.-P. Ye, L. Lin, C.-Q. Liu, C.-C. Chen and Y.-G. Yao, *ChemCatChem*, 2017, **9**, 4587–4597; (l) A. A. Fedorova, I. V. Morozov, Y. N. Kotovshchikov, B. V. Romanovsky, S. V. Sirotnin, E. E. Knyazeva, A. S. Lermontov and A. S. Shaporev, *Mendeleev Commun.*, 2011, **21**, 171–172.
- 15 (a) M. Cortes-Clerget, J. Yu, J. R. A. Kincaid, P. Walde, F. Gallou and B. H. Lipshutz, *Chem. Sci.*, 2021, **12**, 4237–4266; (b) F. Mohajer, M. M. Heravi, V. Zadsirjan and N. Poormohammad, *RSC Adv.*, 2021, **11**, 6885–6925; (c) Y. Baqui, *Catalysts*, 2021, **11**, 46; (d) L. Zhou, S. Li, B. Xu, D. Ji, L. Wu, Y. Liu, Z.-M. Zhang and J. Zhang, *Angew. Chem.*, 2020, **59**, 2769–2775; (e) B. Feng, Y. Yang and J. You, *Chem. Commun.*, 2020, **56**, 790–793; (f) A. S. Díaz-Marta, S. Yañez, E. Lasorsa, P. Pacheco, C. R. Tubío, J. Rivas, Y. Piñeiro, M. A. Gonzalez Gómez, M. Amorín, F. Guitián and A. Coelho, *ChemCatChem*, 2020, **12**, 1762–1771; (g) Y. Tian, J. Wang, X. Cheng, K. Liu, T. Wu, X. Qiu, Z. Kuang, Z. Li and J. Bian, *Green Chem.*, 2020, **22**, 1338–1344; (h) D.-L. Zhu, R. Xu, Q. Wu, H.-Y. Li, J.-P. Lang and H.-X. Li, *J. Org. Chem.*, 2020, **85**, 9201–9212.
- 16 (a) D. Znidar, C. A. Hone, P. Inglesby, A. Boyd and C. O. Kappe, *Org. Process Res. Dev.*, 2017, **21**, 878–884; (b) I. Penafiel, A. Martinez-Lombardia, C. Godard, C. Claver and A. Lapkin, *Sustainable Chem. Pharm.*, 2018, **9**, 69–75; (c) S. Voltrova and J. Srogl, *Org. Chem. Front.*, 2014, **1**, 1067–1071; (d) L.-M. Tan, Z.-Y. Sem, W.-Y. Chong, X. Liu, Hendra, W. L. Kwan and C.-L. Ken Lee, *Org. Lett.*, 2013, **15**, 65–67.
- 17 (a) M. A. Newton, D. Ferri, C. J. Mulligan, I. Alxneit, H. Emerich, P. B. J. Thompson and K. K. Hii, *Catal. Sci. Technol.*, 2020, **10**, 466–474; (b) F. Ferlin, P. M. Luque Navarro, Y. Gu, D. Lanari and L. Vaccaro, *Green Chem.*, 2020, **22**, 397–403; (c) F. Ferlin, M. K. Van der Hulst, S. Santoro, D. Lanari and L. Vaccaro, *Green Chem.*, 2019, **21**, 5298–5305; (d) F. Ferlin, T. Giannoni, A. Zuliani, O. Piermatti, R. Luque and L. Vaccaro, *ChemSusChem*, 2019, **12**, 3178–3184; (e) F. Ferlin, M. Cappelletti, R. Vivani, M. Pica, O. Piermatti and L. Vaccaro, *Green Chem.*, 2019, **21**, 614–626; (f) E. M. Barreiro, Z. Hao, L. A. Adrio, J. R. van Ommen, K. Hellgardt and K. K. Hii, *Catal. Today*, 2018, **308**, 64–70; (g) L. Vaccaro, M. Curini, F. Ferlin, D. Lanari, A. Marrocchi, O. Piermatti and V. Trombettoni, *Pure Appl. Chem.*, 2018, **90**, 21–33; (h) J. B. Brazier, B. N. Nguyen, L. A. Adrio, E. M. Barreiro, W. P. Leong, M. A. Newton, S. J. A. Figueroa, K. Hellgardt and K. K. Hii, *Catal. Today*, 2014, **229**, 95–103.
- 18 (a) Y. Mohr, M. Alves-Favaro, R. Rajapaksha, G. Hisler, A. Ranscht, P. Samanta, C. Lorentz, M. Duguet, C. Mellot-Draznieks, E. A. Quadrelli, F. M. Wisser and J. Canivet, *ACS Catal.*, 2021, **11**, 3507–3515; (b) S. Checchia, C. J. Mulligan, H. Emerich, I. Alxneit, F. Krumeich, M. Di Michiel, P. B. J. Thompson, K. K. Hii, D. Ferri and M. A. Newton, *ACS Catal.*, 2020, **10**, 3933–3944; (c) F. Ferlin, S. R. Yetra, S. Warratz, L. Vaccaro and L. Ackermann, *Chem. – Eur. J.*, 2019, **25**, 11427–11431; (d) F. Ferlin, L. Luciani, O. Viteritti, F. Brunori, O. Piermatti, S. Santoro and L. Vaccaro, *Front. Chem.*, 2019, **6**, 659.
- 19 (a) F. Valentini, H. Mahmoudi, L. A. Bivona, O. Piermatti, M. Bagherzadeh, L. Fusaro, C. Aprile, A. Marrocchi and L. Vaccaro, *ACS Sustainable Chem. Eng.*, 2019, **7**, 6939–6946; (b) H. Mahmoudi, F. Valentini, F. Ferlin, L. A. Bivona, I. Anastasiou, L. Fusaro, C. Aprile, A. Marrocchi and L. Vaccaro, *Green Chem.*, 2019, **21**, 355–360; (c) F. Ferlin, L. Luciani, S. Santoro, A. Marrocchi, D. Lanari, A. Bechtoldt, L. Ackermann and L. Vaccaro, *Green Chem.*, 2018, **20**, 2888–2893; (d) E. Petricci, C. Risi, F. Ferlin, d. Lanari and L. Vaccaro, *Sci. Rep.*, 2018, **8**, 10571; (e) F. Ferlin, S. Santoro, L. Ackermann and L. Vaccaro, *Green Chem.*, 2017, **19**, 2510–2514; (f) G. Rubulotta, K. L. Luska, C. A. Urbina-Blanco, T. Eifert, R. Palkovits, E. A. Quadrelli, C. Thieuleux and W. Leitner, *ACS Sustainable Chem. Eng.*, 2017, **5**, 3762–3767.
- 20 (a) F. Valentini and L. Vaccaro, *Molecules*, 2020, **25**, 5264; (b) D. Rasina, A. Lombi, S. Santoro, F. Ferlin and L. Vaccaro, *Green Chem.*, 2016, **18**, 6380–6386; (c) F. Ferlin, V. Trombettoni, L. Luciani, S. Fusi, O. Piermatti, S. Santoro and L. Vaccaro, *Green Chem.*, 2018, **20**, 1634–1639.
- 21 F. Trotta, K. Martina, B. Robaldo, A. Barge and G. Cravotto, *J. Inclusion Phenom. Macrocyclic Chem.*, 2007, **57**, 3–7.

- 22 U. I. Kramm, R. Marschall and M. Rose, *ChemCatChem*, 2019, **11**, 2563–2574.
- 23 (a) H. Xie, L. Ming, J. Wu, Y. Zhang and Y. Cheng, WO2020/114494A1, 2020; (b) C. N. Jain, M. N. Vaghela, R. B. Rehani and R. Thenati, WO2006/059345A2, 2006; (c) M. E. Garst, L. J. Dolby and N. A. Fedoruk, US005420295A, 1995.
- 24 J. Andraos, *Green Process. Synth.*, 2019, **8**, 324–336, DOI: 10.1515/gps-2018-0131.
- 25 J. Andraos, *Org. Process Res. Dev.*, 2013, **17**, 175–192.